

Potential failure mode identification of operational amplifier circuit board by using high accelerated limit test

Junji Sakamoto^a, Ryoma Hirata^b, and Tadahiro Shibutani^{c*}

^a *Institute of Advanced Sciences, Yokohama National University, 79-5 Tokiwadai, Hodogaya-ku, Yokohama, Kanagawa 240-8501, Japan*

^b *Graduate School of Environment and Information Sciences, Yokohama National University, 79-7 Tokiwadai, Hodogaya-ku, Yokohama, Kanagawa 240-8501, Japan*

^c *Center for Creation of Symbiosis Society with Risk, Yokohama National University, 79-5 Tokiwadai, Hodogaya-ku, Yokohama, Kanagawa 240-8501, Japan*

* Corresponding author

Tel: +81-45-339-3597, E-mail: shibutani-tadahiro-bj@ynu.ac.jp

Abstract

In this study, the potential failure modes of a small operational amplifier circuit board were investigated. The high accelerated limit test (HALT) was employed to identify the failure modes under multi-axial vibration and temperature loadings. Five stress tests, specifically, low and high temperature, vibration, thermal shock, and composite profiles were performed. An aluminum electrolytic capacitor was damaged under the low temperature process, whereas the capacitance of a ceramic capacitor decreased under the high temperature process. The vibration test revealed that mechanical fatigue occurs at the terminal leads of aluminum electrolytic capacitors. The HALT also revealed coupled effects between high and low temperature processes and vibration.

Keywords: high accelerated limit test, operational amplifier circuit board, potential failure mode.

1. Introduction

The Internet of Things (IoT) offers a new paradigm in the modern social system and the global market is expanding [1]. The major concern regarding the increasing number of connected devices is reliability of the electronic products. Reliability is the ability of an item to perform under expected performance requirements for a specified period in field-use conditions and the classic frequency approach is currently applied to ensure product reliability. However, the significant increase in the number of connected devices suggests that the classic approach will soon become ineffective; therefore, new technology to assess the reliability of systems is required.

Reliability tests are an effective way to verify the design of products. The thermal cycling test is a typical design verification test for interconnections such as solder joints. Thermo-mechanical fatigue of the interconnections is a major failure mechanism and the test conditions are also designed based on the target failure mechanism. However, even in cases where products passed the thermal cycling reliability test,

1 failures have occurred in the field. This implies that some potential failure modes are beyond the scope of
2 the reliability test employed. There are many components on a circuit board owing to the trend toward highly
3 integrated technology in electronics. The potential risk of electronic products is consequently increasing.

4 The prognostic health management (PHM) can be an effective solution for diagnosing failures, predicting
5 residual lifetime, and estimating the reliability of assets [2]. PHM consists of sensing, diagnose, prognosis,
6 and management stages. A key feature of PHM is its failure criteria. These failure criteria are determined by
7 the physics-of-failure or sensing data trends.

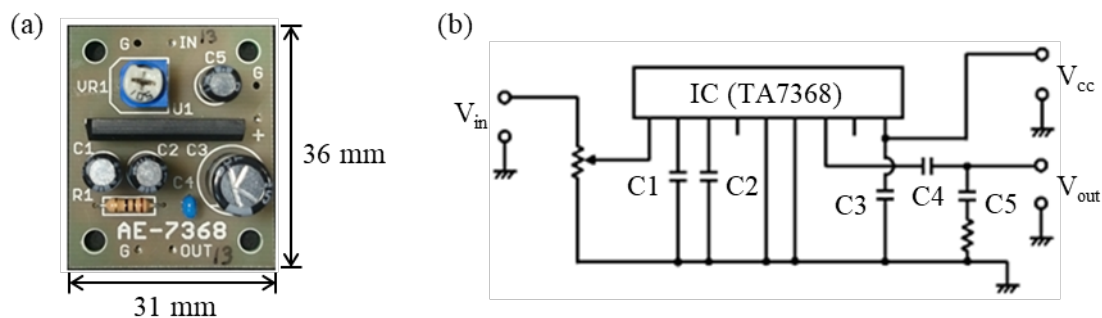
8 The high accelerated limit test (HALT) is a method that identifies the weakness of systems such as
9 electronic products [3]. In this test, severe temperature/vibration stresses beyond the specified operating
10 limits are applied to the product. HALT can be used to provide threshold determination such as the
11 operational limit and the destruct limit of products. IPC 9592A provides the requirements for HALT [4].

12 This paper reports on a study in which the failure modes of a small operational amplifier circuit board
13 were investigated using HALT. First, failure mode and effect analysis (FMEA), which is a qualitative method
14 to extract the typical failure modes of products, was applied to extract their potential failure modes and their
15 effects before HALT. HALT was subsequently performed on an operational amplifier circuit board to
16 investigate its potential failure modes.

17 2. Experimental procedure

18 2.1 Failure mode and effect analysis of operational amplifier circuit board

19 This section explains the FMEA procedure performed to extract potential failure modes and their effects
20 before application of HALT. Figure 1 presents a schematic of the operational amplifier circuit board used
21 (Akizuki Denshi Tsusho Co., Ltd., AE-7368). The following test components were used: operational
22 amplifier IC (TA7368), aluminum electrolytic capacitors (C1, C2, C3, and C5), ceramic capacitor (C4), and
23 resistances (VR). These components were connected to the circuit board using tin-lead solder.



26
27 **Figure 1 The tested circuit board: (a) circuit board and components; (b) circuit diagram.**

28
29 FMEA is a systematic method for identifying potential failure modes and prioritizing them. In this study, the
30 failure modes of components were open circuit and short circuit [5], [6]. Further, decreasing capacitance and
31 increasing leakage current were also considered for capacitors. The effect of each failure mode was

1 investigated per component using a breadboard before manufacture. Table 1 summarizes the results of FMEA
 2 for the small operational amplifier circuit components.

3

4 Table 1 Failure modes and effect analysis of small operational amplifier circuit board components.

Component	ID	Failure mode	Anomaly of output voltage
Aluminum capacitor	C1	Open circuit	Decrease to 0 V
		Short circuit	No change
		Capacitance decrease	No change
		Increase in leakage current	Decrease slowly to 0 V
	C2	Open circuit	No amplitude with noise
		Short circuit	No amplitude
		Capacitance decrease	Amplitude reduction
		Increase in leakage current	Increase slowly to 5.0 V
	C3	Open circuit	No signal (0 V)
		Short circuit	Shift to 4.0 V
		Capacitance decrease	Amplitude reduction
		Increase in leakage current	Shift slowly to 4.0 V
	C5	Open circuit	Rectangular wave and noise
		Short circuit	No signal (0 V)
		Capacitance decrease	Rectangular wave and noise
		Increase in leakage current	No change
Ceramic capacitor	C4	Open circuit	No change
		Short circuit	Shift to 0 V
		Capacitance decrease	No change
		Increase in leakage current	Shift to 0 V
Trimmer potentiometer	VR	Open circuit (INPUT)	No amplitude
		Open circuit (GND)	Rectangular wave
		Short circuit (INPUT)	Rectangular wave
		Short circuit (GND)	No amplitude

5

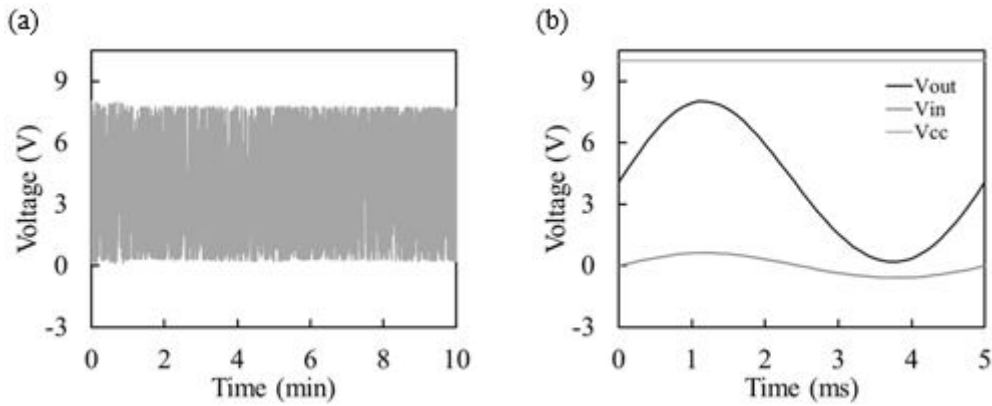
6 2.2 Test procedure for HALT chamber

7 In this study, eighteen circuit boards (No. 1 to No. 18) were prepared for HALT. Groups of three circuit
 8 boards were mounted on an aluminum plate (150 mm × 150 mm × 2 mm). Therefore, six specimen groups
 9 (A to F) were tested in several stress step recipes. A 10 V voltage collector was applied to each circuit using
 10 a power supply (Matsusada Precision Inc., PK-80). A 200 Hz sine wave with amplitude 0.6 V was generated
 11 as input voltage. Input and output voltages data acquisition was performed using LabView with a sampling
 12 rate of 5 S/sec. The sine waveform during the HALT steps was captured every ten seconds at a sampling rate
 13 of 10 kS/sec. Figure 2 shows examples of the output voltage (V_{out}), input voltage (V_{in}), and voltage collector

1 (V_{cc}) at the sampling rates of 5 S/sec and 10 kS/sec.

2

3



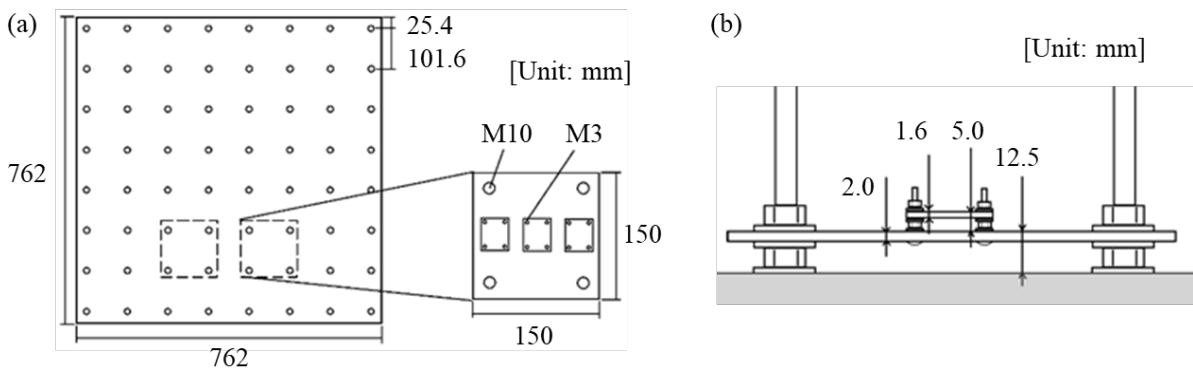
4

5 **Figure 2 Sample voltages (V_{out} , V_{in} , V_{cc}) for sampling rates of (a) 5 S/sec and (b) 10 kS/sec.**

6

7 The Qualmark Typhoon 2.5 HALT chamber, which provides controlled temperature and vibration to the
8 product, was used in this study. The rapid temperature change rate (60 °C /minute) and severe vibration tests
9 were conducted with two test specimens fixed to a 762 mm² shaking table. Figure 3 shows the setup of the
10 specimens on the shaking table.

11



12

13 **Figure 3 Setup of specimens on the HALT shaking table: (a) Top view; (b) side view**

14

15 HALT can provide the following five kinds of stress tests to a specimen [6], [7], [8]:

16 1. Low temperature stress

17 2. High temperature stress

18 3. Vibration stress

19 4. Thermal shock stress

20 5. Combined temperature-vibration stresses

21

22 Specimen groups A (No. 1, No. 2, No. 3) and C (No. 7, No. 8, No. 9) were tested in the low temperature

1 stress test. The test started at 20 °C and the chamber temperature decreased by 10 °C until functional failure
2 occurred. Specimen groups B (No. 4, No. 5, No. 6) and C were tested in the high temperature stress test. The
3 chamber temperature was increased by 10 °C. Specimen group and D (No. 10, No. 11, No. 12) were tested
4 in the vibration stress test. The vibration level was increased by 10 G_{rms} and its holding time, including
5 transition time, was 10 minutes. Specimen group C was thus tested under low temperature/high
6 temperature/vibration stresses. Comparing specimen groups A, B, C, and D, the effect of accumulated
7 damage on product failure was examined. Specimen group E (No. 13, No. 14, No. 15) was evaluated for
8 thermal shock stress. The test condition of thermal shock was determined by the results of low/high
9 temperature stresses. Specimen group F (No. 16, No. 17, No. 18) was evaluated for combined temperature-
10 vibration stress. The test condition was considered based on the result of the vibration stress step.

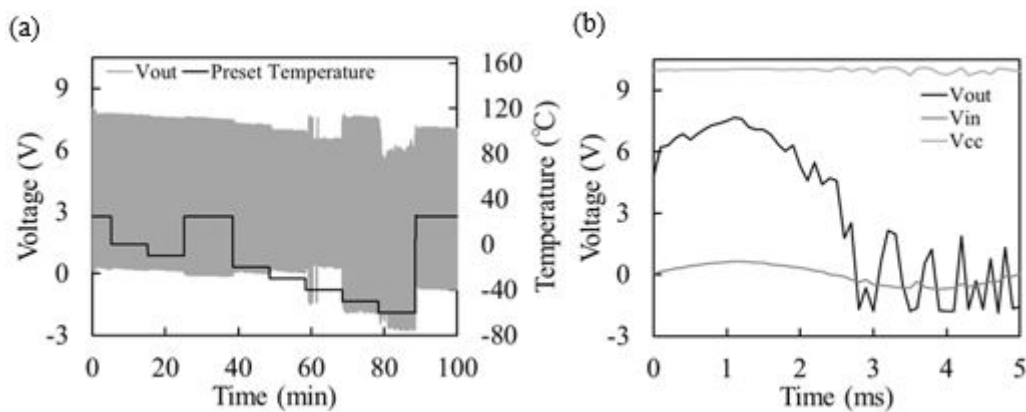
11

12 3. Results

13 3.1 Low temperature stress test

14 As temperature decreases, the amplitude of the output voltage of an amplifier becomes narrower. It is well-
15 known that the electrostatic capacity of an aluminum electrolytic capacitor tends to decrease at low
16 temperatures [9]. In this circuit board, the capacitor (C2) may affect the change in the amplitude of output
17 voltage based on FMEA. The temperature in the chamber was decreased to -60 °C and the output waveform
18 was seen to have a noise irregularity at -50 °C. Figure 4 shows the noised wave of the output voltage at -
19 50 °C. The output voltage fell at -60 °C, resulting in reduced performance by the ceramic capacitor. Based
20 on FMEA, the reduced performance of the aluminum capacitor (C5) induced noise in the output waveform.
21 In this study, the lower operating limit (LOL) of this circuit was thus identified as -50 °C.

22



23

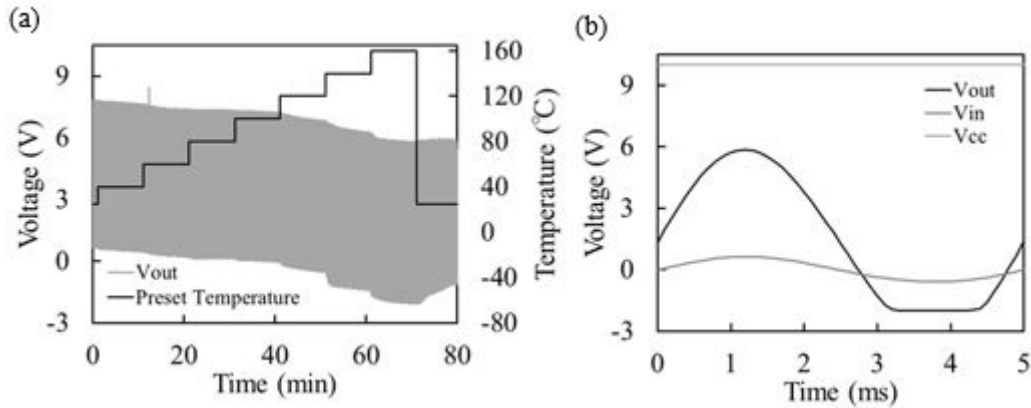
24 **Figure 4 Output voltages in the low temperature stress test: (a) monitoring at 5 S/sec; waveform at -**
25 **50 °C**

26

27 3.2 High temperature stress step

28 The average output voltage is decreased as the temperature of the chamber increased during the high
29 temperature test. The capacitance of the ceramic capacitor used in this study decreases with increasing
30 temperature. In the high temperature stress test, the temperature was increased to a maximum of 160 °C.

1 Figure 5 shows the output voltage with 10 kS/sec at 160 °C. It can be seen that the output voltage does not
 2 maintain the sine waveform. We also conducted leakage current analysis of the circuit board. The leakage
 3 current of the aluminum capacitor C1 provided a similar profile as that in Figure 5. Then, the leakage current
 4 of C1 may be a potential failure mode in the high temperature stress test for the upper operating limit (UOL)
 5 in this study of 160 °C.
 6



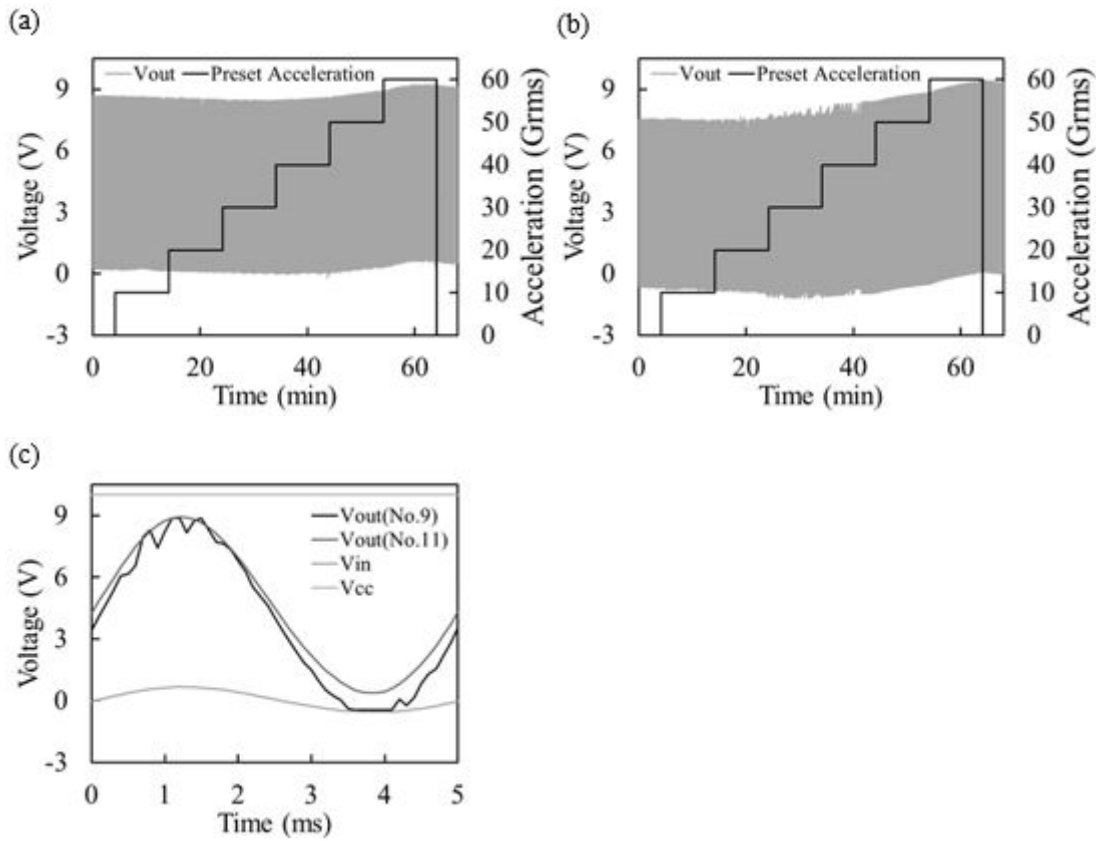
7
 8 **Figure 5 Output voltages for high temperature stress step: (a) monitoring at 5 S/sec; (b) waveform at**
 9 **160 °C**

10

11 **3.3 Vibration stress step**

12 In the vibration test, the output voltage increased with the vibration level. The leakage current analysis
 13 revealed that the increase in output voltage occurred because of the leakage current of aluminum electrolytic
 14 capacitor C2 or C3. When the vibration level reached 30 G_{rms} , the output voltage had a noise irregularity.
 15 The vibration stress test was conducted up to 60 G_{rms} . The output voltage at 60 G_{rms} is shown in Figure 6.
 16 After the experiment, leakage of electrolyte solution was found at aluminum electrolytic capacitor C3 on the
 17 No. 9 circuit board, as shown in Figure 7. There are two possible failure modes in the vibration stress test:
 18 (1) intermittent electrical short of aluminum capacitor C3; (2) open circuit in the trimmer potentiometer.
 19 Comparing Specimen groups C and D, circuit board failure (No. 7, No. 8, No. 9) occurred earlier in specimen
 20 group C than in specimen group D. This implies that the low/high temperature stress test in the case of
 21 specimen group C resulted in damage to the circuit boards.

22



1

2

3 **Figure 6 Output voltages for vibration stress test: Monitoring at 5 S/sec for No. 9; Monitoring at 5**
 4 **S/sec for No. 11; Waveforms at 60 Grms**

5



6

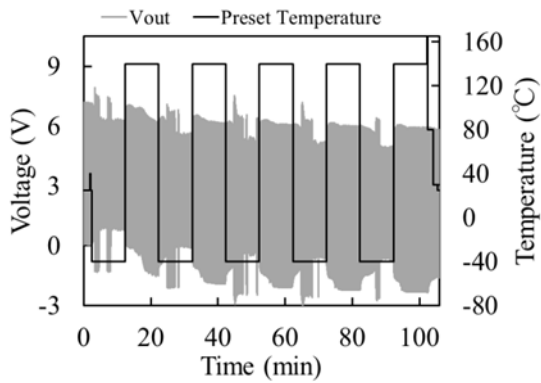
7 **Figure 7 Failure at aluminum capacitor C3 after vibration stress test (No. 9 circuit board).**

8

9 **3.4 Thermal shock test**

10 On the basis of the results of the high and low temperature stress tests, the upper and lower temperatures
 11 used in this test were 140 and -40 °C, respectively. Figure 8 shows the output voltage obtained during the
 12 thermal shock step. Similar failure modes as in the low and high temperature stress tests were observed in

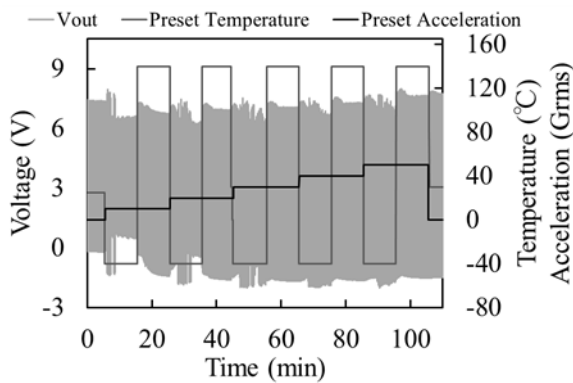
1 the thermal shock step. The output voltage decreased with thermal cycling.
2



3
4 **Figure 8 Output voltage monitoring for thermal shock stress test.**

5
6 **3.5 Combined stress test**

7 Figure 9 shows the output voltage obtained during the combined stress test. When the vibration level was
8 less than 30 Grms, the average output voltage did not increase. As the vibration level increased above 30 Grms,
9 the average amplitude of the output voltage increased. This is the combined effect of high/low temperature
10 and vibration stress steps.
11



12
13 **Figure 9 Output voltage monitoring for combined stress test.**

14
15 **4. Discussion**

16 Most of the behavior observed in HALT is associated with the temperature dependency of the components
17 on the circuit boards. In general, the electrical capacity of the aluminum capacitor and the ceramic capacitors
18 decreases at low temperature. In addition, the capacitance of ceramic capacitors tends to decrease at high
19 temperatures.

20 Another failure mode is the leakage current of components. In this study, the typical failure modes of the
21 components were open circuit and electrical short in the FMEA. The leakage current of each component was
22 analyzed via a circuit board diagram and the failure mode of leakage current added.

23 Another finding is the interaction between the five tests in the HALT. In general, the five stress tests were
24 performed step by step in the HALT chamber. However, the interaction problem between temperature and

1 vibration steps is still not clear. In this study, the history of test steps was also investigated. The vibration
2 test history revealed that some components were damaged under the high/low temperature tests.

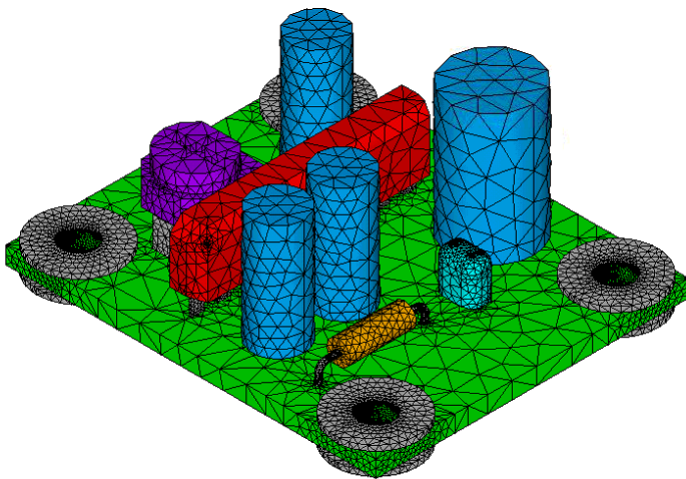
3 Finite element mode analysis was also performed to investigate the failure mechanism in the vibration
4 stress test [9]. The commercial structural analysis software ANSYS 16.0 was used. The finite element model
5 is shown in Figure 10. Table 2 lists the material properties of the components used in the analysis. The
6 Young's modulus and Poisson's ratio of the components were obtained from the references. The Poisson's
7 ratio of the IC, ceramic capacitor, and trimmer potentiometer was assumed to be 0.3. The density of each
8 component was calculated using the weight of the component and its volume from CAD data. Washers were
9 glued to the circuit board and the upper and lower surfaces of the washers were fixed. Mode analysis was
10 performed over a frequency range of 0 to 5000 Hz.

11

1 **Table 2 Material properties of the components used in the finite element analysis.**

	Young's modulus [GPa]	Poisson's ratio [-]	Density [kg/m ³]	Number of nodes [-]	Number of elements [-]
Printed circuit board (FR4)	24.3 [11]	0.30	1800	111356	66526
Lead pin (Alloy42)	145 [12]	0.30	8110	-	-
IC	14.0 [13]	0.30	2180	11921	6088
Aluminum capacitor (C1, C2, C5)	68.3 [14]	0.34	1670	7359	4234
Aluminum capacitor (C3)	68.3	0.34	1590	6906	4014
Ceramic capacitor (C4)	180 [15]	0.30	650	10324	6222
Trimer potentiometer (VR)	2.4 [16]	0.30	1640	5756	3006
Washer (M3, SUS304)	193 [17]	0.30	7930	6805	3282

2

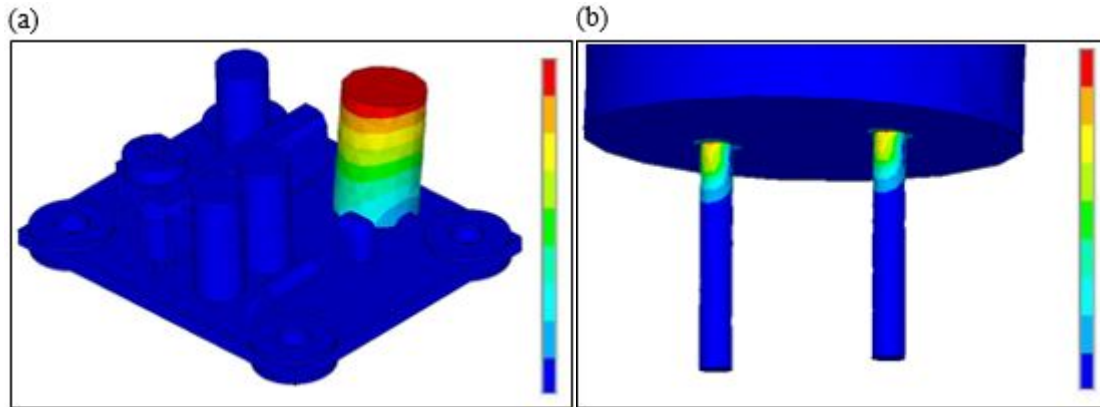


3

4 **Figure 10 Finite element model of the operational amplifier circuit board.**

5

1 The lowest excitation mode frequency was 867 Hz. The deformation mode at 867 Hz is shown in Figure
2 11. The aluminum capacitor C3 was the excited component. This agrees with the observed failure mode in
3 the vibration stress test and the results of other studies [9]. Therefore, the failure mechanism of the vibration
4 stress test is mechanical fatigue of the lead pins for aluminum capacitor C3.



6
7 **Figure 11 Modal analysis results for the operational amplifier circuit board. Excitation of C3 occurred**
8 **at 867 Hz. (a) Displacements; equivalent stress**

9 **5. Conclusions**

10 In this study, the failure modes of a small operational amplifier circuit board were assessed using the high
11 accelerated limit test (HALT). Several failure modes were observed for five types of stress tests.

12 1) FMEA can extract the typical failure modes of small operational amplifier circuit boards, and thus can be
13 a useful tool for screening failure modes.

14 2) The failure modes depend on the temperature sensitivity of the mounted components in the high and low
15 temperature tests.

16 3) The vibration test can identify weak components because of the natural frequency of the circuit board.
17 Finite element analysis can predict the result of the vibration test.

18 4) The temperature test may affect the vibration test. The accumulated damage of components accelerates
19 the failure in the vibration test.

20 **Acknowledgements**

21 Authors would thank for the consortium of HALT-based high-quality design.

22 **References**

- 23 [1] J. Gubbi, R. Buyya, S. Marusic, M. Palaniswami, "Internet of Things (IoT): A vision, architectural
24 elements, and future directions," *Future Generation Computer Systems*, Vol. 29, pp. 1645-1660, 2013.
25 [2] D. Kwon, M. R. Hodkiewicz, J. Fan, T. Shibutani, M. G. Pecht, "IoT-based prognostics and systems
26 health management for industrial applications," *IEEE Access*, Vol. 4, pp. 3659-3670, 2016/07.

- 1 [3] K. A. Gray, J. J. Paschkewitz, Next generation HALT and HASS, Wiley, 2016.
- 2 [4] IPC, Requirements for Power Conversion Devices for the Computer and Telecommunications
3 Industries, IPC-9592A, 2010.
- 4 [5] H. S.-H. Chung, H. Wang, F. Blaabjerg, M. Pecht, Reliability of power electronic converter systems,
5 The Institution of Engineering and Technology, 2016.
- 6 [6] H. Chen, B. Yao, Q. Xiao, “The study on application of HALT for DC/DC converter,” Proceedings
7 of 2014 International Conference on Reliability, Maintainability and Safety (ICRMS), 2014.
- 8 [7] Qualmark, HALT Testing Guidelines, 2014.
- 9 [8] M. Catelani, L. Ciani, “Highly accelerated life testing for avionics devices,” Proceedings of the
10 International Conference on Metrology for Aerospace, 2014.
- 11 [9] Rubycon Corporation, Technical notes for electrolytic capacitor,
12 <http://rubycon.co.jp/en/products/alumi/pdf/Performances.pdf> (Accessed 23 September 2017).
- 13 [10] E. Habtour, W. Connon, M. F. Pohland, S. C. Stanton, M. Paulus, A. Dasgupta, “Review of response
14 and damage of linear and nonlinear systems under multi-axial vibration,” Shock and Vibration, Article
15 ID 294271 (21 pages), 2014
- 16 [11] Hirose, <http://www.hirosugi.co.jp/technical/material/GG.html> (Accessed 2 June 2017).
- 17 [12] Furukawa Electric, High performance copper alloys for leadframe,
18 http://www.furukawa.co.jp/product/catalogue/pdf/leadframe_s133.pdf (Accessed 2 June 2017).
- 19 [13] Shinetsu, http://www.shinetsu-encap-mat.jp/product/k_s/kmc/ (Accessed 2 June 2017).
- 20 [14] Aluminium Today, <https://www.aluminum.or.jp/basic/aluminumtoha/fset1.html> (Accessed 2 June
21 2017).
- 22 [15] Kyocera, Characteristics of Kyocera fine ceramics,
23 <http://www.kyocera.co.jp/prdct/fc/product/pdf/material.pdf> (Accessed 2 June 2017).
- 24 [16] Kayo Corporation, http://www.kayo-corp.co.jp/common/pdf/pla_propertylist01.pdf (Accessed 2 June
25 2017).
- 26 [17] Japan Stainless Steel Association, <http://www.jssa.gr.jp/contents/faq-article/q6/> (Accessed 2 June 2017).
- 27